JOURNAL OF MATERIALS SCIENCE **36** (2001) 2991 – 2997

Incorporation of bismuth into $Ba_{6-x}R_{8+2/3x}Ti_{18}O_{54}$ (R = Nd, Gd)

MATJAZ VALANT, DANILO SUVOROV
Jozef Stefan Institute, Jamova 39. 1000 Ljubljana, Slovenia

Microstructural investigations and microanalyses of a series of $Ba_{6-x}R_{8+2/3x}Ti_{18}O_{54}$ ceramics (R = Nd, Gd) revealed that the solid-solubility limit for the isovalent substitution of R^{3+} by Bi^{3+} depends on the composition of the $Ba_{6-x}R_{8+2/3x}Ti_{18}O_{54}$ phase. For the Nd analogue the solid-solubility limit (y in $Ba_{6-x}(Nd_{1-y}Bi_y)_{8+2/3x}Ti_{18}O_{54}$) decreases with a decrease in x from $y = 0.16$ for $x = 2.0$ to $y = 0.10$ for $x = 0.8$. An even lower solid-solubility limit ($y = 0.06$) was found for the $Ba_{4.5}(Gd_{1-y}Bi_y)_9Ti_{18}O_{54}$ compound ($x = 1.5$). All substituted Nd compositions exhibit higher permittivities (93–99), lower temperature coefficients of permittivity (11–15 ppm/K) and higher dielectric losses ($Q \cdot f$ = 1300–5500 GHz) than the parent compositions. By exceeding the solid-solubility limit, abrupt changes in the microstructural and dielectric characteristics are induced.

1. Introduction

High permittivity ceramics used in up-to-date microwave systems are mainly based on solid solutions, with a general formula $Ba_{6-x}R_{8+2/3x}Ti_{18}O_{54}$ (R = La–Gd). Although all rare-earth ions from La to Gd form this type of crystal structure, the majority of high-permittivity microwave ceramic components are manufactured from the Nd analogue, because it has the most suitable dielectric properties.

The crystal structure of $Ba_{6-x}R_{8+2/3x}Ti_{18}O_{54}$ solid solutions includes elements of tungsten bronze with channels extending in the short-axis direction [1, 2]. Corner-sharing TiO_6 octahedra form a network with three types of channels: pentagonal, rhombic, and triangular. Rare-earth ions occupy the rhombic channels, Ba ions completely fill the pentagonal channels (for $x < 2$), while the remaining Ba ions share the rhombic channels. The triangular channels are empty [3]. Although some details regarding the homogeneity range still remain unclear, most researchers agree that x for La is $0.2 < x < 2.3$, [4] for Pr $0 < x < 2.25$, [5, 6] for Nd $0 < x < 2.1$ ($0 > x > 0.7$ for $Ba_{6-3x}Nd_{8+2x}Ti_{18}O_{54}$ formula) [7] or $0.6 < x < 2.1$ [8], for Sm $0.9 < x < 2.1$ [7, 8] ($0.3 > x > 0.7$ for $Ba_{6-3x}Sm_{8+2x}Ti_{18}O_{54}$ formula [7]) for Eu = $1.2 < x < 1.5$, [8] and for Gd $x = 1.5$ [9].

The major task in the development of $Ba_{6-x}Nd_{8+2/3x}Ti_{18}O_{54}$-based ceramics is to suppress the high positive temperature coefficient of resonant frequency (τ_f) and increase the permittivity. Several different concepts of dielectric-property modification [10] can be applied for $Ba_{6-x}Nd_{8+2/3x}Ti_{18}O_{54}$; one of them is isovalent substitution. To optimize the substitution and to obtain the best improvement in the microwave dielectric properties by a particular substituent, the mechanism of its incorporation into the crystal structure of $Ba_{6-x}Nd_{8+2/3x}Ti_{18}O_{54}$ must be understood.

It has already been shown that the microwave dielectric properties of $Ba_{6-x}Nd_{8+2/3x}Ti_{18}O_{54}$ can be effectively tailored by doping with bismuth [8, 11]. Studies of the isovalent Bi substitution revealed that Bi^{3+} substitutes for Nd^{3+} in the crystal structure of $Ba_{4.5}Nd_9Ti_{18}O_{54}$. The EXAFS studies of Bi-substituted $Ba_{4.5}Nd_9Ti_{18}O_{54}$ [12] revealed that Bi^{3+} does not substitute for Nd^{3+} randomly on all possible sites but rather selectively enters one of three possible channels, i.e. the site $x = 0.9484$, $y = 0.2500$, $z = 0.2939$ and/or $x = 0.0455$, $y = 0.2500$, $z = 0.6928$ previously occupied by Nd^{3+} [13]. The saturated phase can be written as $Ba_{4.5}(Nd_{0.85}Bi_{0.15})_9Ti_{18}O_{54}$. After exceeding the solid solubility limit, additional Bi_2O_3 concentrates as a Bi-rich phase at the grain boundaries, causing considerable reduction of the Q-value and an increase in the τ_f of such ceramics [11].

The aim of this study is to extend the investigations of the Bi incorporation, described in the literature [11], on the wide range of the isostructural $Ba_{6-3x}R_{8+2/3x}Ti_{18}O_{54}$ solid solutions. The investigations are intended to reveal parameters of the Bi incorporation in two basic directions of the $Ba_{6-3x}R_{8+2x}Ti_{18}O_{54}$ solid-solution region; the Bi incorporation was studied as a function of x and R.

2. Experimental procedure

Samples were prepared by solid-state reaction. Reagent-grade Bi_2O_3, $Nd_2O_3 \cdot 2TiO_2$, $BaTiO_3$ and TiO_2 were wet mixed and calcined at 1150°C for 6 hours. The material was then wet milled to a particle size around 1 μm. For microwave measurements, powders were uniaxially pressed into disks under a pressure of 100 MPa. The samples were sintered at 1320–1340°C for 20 minutes in an air atmosphere.

Microstructures of the samples were characterized by scanning electron microscopy (SEM) (JEOL, Model JXA 840A, Tokyo, Japan) and quantitative microanalysis was performed by wavelength dispersive spectroscopy (WDS) or energy-dispersive X-ray spectroscopy (EDX) using TRACOR software (Tracor Northern, Model NORAN TRACOR Series II X-Ray Microanalyser, Middleton, USA). Identification of the phases was performed by X-ray diffraction (Philips, Model PW 1710, Bedrijven b. v. S&I, Netherlands). Microwave dielectric properties were measured by a Network Analyzer (HP, Model HP 8719C, Santa Rosa, USA) applying the reflection-resonant-cavity method.

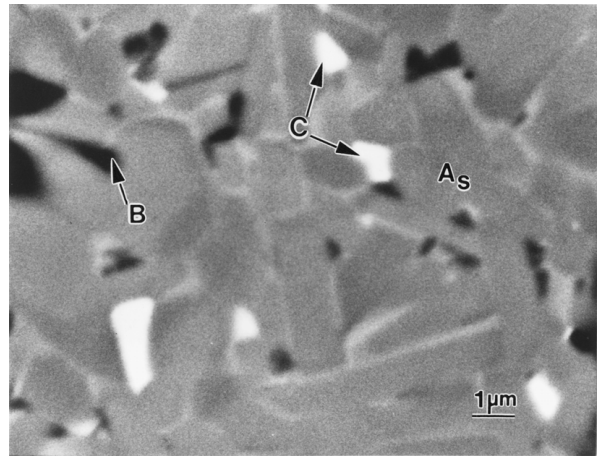

Figure 2 Back-scattered electron image of the polished surface of the ceramics with the nominal composition $Ba_4(Nd_{1-y}Bi_y)_{9.33}Ti_{18}O_{54}$ ($y = 0.225$): pre-reacted 10 h at 1200°C and sintered 20 min at 1320°C (A_s...saturated Bi-doped $Ba_4Nd_{9.33}Ti_{18}O_{54}$, B...$TiO_2$, C...Bi-rich phase).

3. Results

The investigations of the solid-solubility limit of Bi incorporation in $Ba_{6-x}R_{8+2x/3}Ti_{18}O_{54}$ were conducted for the three different representatives: two $Ba_{6-x}Nd_{8+2x/3}Ti_{18}O_{54}$ representatives, one from the high-x ($x = 2.0$) and one from the low-x side ($x = 0.8$) of the homogeneity range, and $Ba_{4.5}Gd_9Ti_{18}O_{54}$.

3.1. Bi incorporation in $Ba_4Nd_{9.33}Ti_{18}O_{54}$ ($x = 2.0$)

The synthesis of the Bi-substituted $Ba_4Nd_{9.33}Ti_{18}O_{54}$ compositions was performed according to the compositional model $Ba_4(Nd_{1-y}Bi_y)_{9.33}Ti_{18}O_{54}$ with nominal y in the range from 0 to 0.25. Microstructural SEM investigations revealed that all $Ba_4(Nd_{1-y}Bi_y)_{9.33}Ti_{18}O_{54}$ ceramics contain, in addition to the Bi-doped $Ba_4Nd_{9.33}Ti_{18}O_{54}$ matrix, a secondary phase which was identified as TiO_2 (Fig. 1). The concentration of the TiO_2 phase increases only slightly up to $y = 0.19$, while a significant increase was observed for $y > 0.19$ ceramics. Additionally, another phase appears in the microstructure of the $y > 0.19$ ceramics. Fig. 2 shows the presence of the Bi-rich phase, which concentrates at the grain boundaries.

WDS microanalyses, performed on the grains of the matrix phase, shows that the actual concentration of bismuth ($y_{anal.}$), which is different than the nominal value due to the loss of Bi during heat treatment, increases with y and reaches the value $y_{anal.} = 0.16$ (± 0.007) at $y = 0.19$. For $y \geq 0.19$ samples $y_{anal.}$ remains constant (Fig. 3). The WDS analyses also revealed the changes in the composition of the matrix phase. In the ceramics with the nominal composition $Ba_4(Nd_{1-y}Bi_y)_{9.33}Ti_{18}O_{54}$ ($y = 0.19$) the composition of the matrix phase moved toward a higher Ba concentration i.e. from $x = 2$ to $x_{anal.} = 1.9$ (± 0.05).

The results of dielectric property measurements show the significant influence of bismuth concentration on the microwave dielectric properties of the ceramics with the nominal composition $Ba_4(Nd_{1-y}Bi_y)_{9.33}Ti_{18}O_{54}$ (Table I). The permittivity increases with an

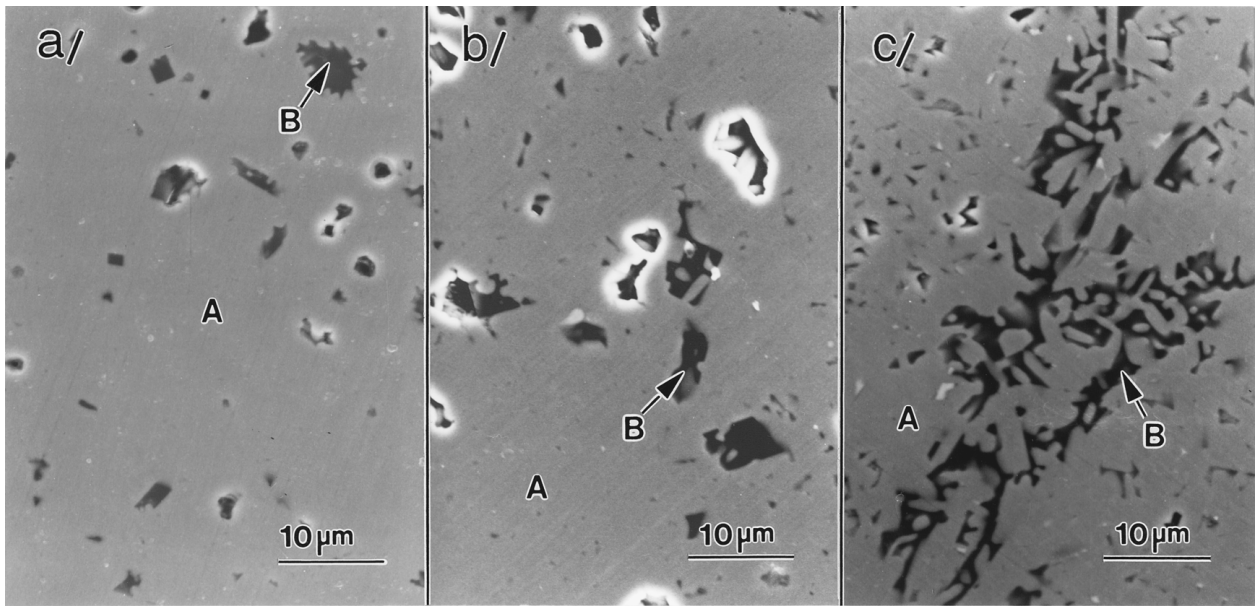

Figure 1 SEM images of the polished surface of the ceramics with the nominal composition $Ba_4(Nd_{1-y}Bi_y)_{9.33}Ti_{18}O_{54}$ ($y = 0.10$ (a), $y = 0.17$ (b) and $y = 0.225$ (c)): pre-reacted 10 h at 1200°C and sintered 20 min at 1320°C (A...Bi-doped $Ba_4Nd_{9.33}Ti_{18}O_{54}$, B...$TiO_2$).

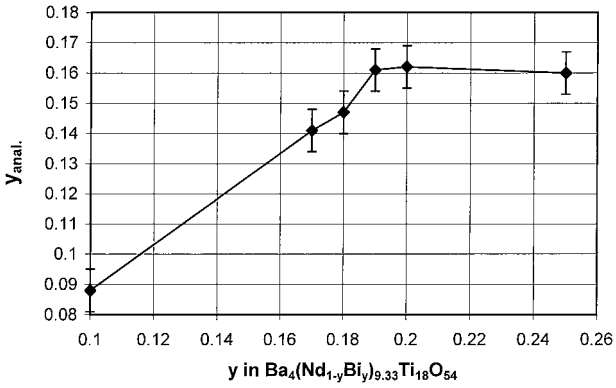

Figure 3 Analyzed (WDS) concentration of bismuth ($y_{anal.}$) in the grains of the matrix phase as a function of nominal bismuth concentration (y) in the $Ba_4(Nd_{1-y}Bi_y)_{9.33}Ti_{18}O_{54}$ ceramics: pre-reacted 10 h at 1200°C and sintered 20 min at 1320°C.

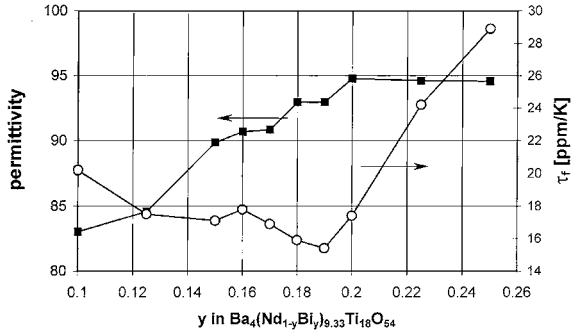

Figure 4 Permittivity and temperature coefficient of resonant frequency as a function of the of nominal bismuth concentration (y) in the $Ba_4(Nd_{1-y}Bi_y)_{9.33}Ti_{18}O_{54}$ ceramics: pre-reacted 10 h at 1200°C and sintered 20 min at 1320°C.

increase in the Bi concentration from 83.0 ($y = 0.10$) to 94.8 (for $y = 0.2$), where it reaches a plateau (Fig. 4). The temperature coefficient of the resonant frequency decreases with an increase in y and reaches the minimum value of 15.4 ppm/K for the $y = 0.19$ sample. With a further increase in y, τ_f increases sharply. Dielectric losses increase monotonously over the entire y-range investigated.

TABLE I Compositional parameters and dielectric properties of the ceramics with nominal composition $Ba_4(Nd_{1-y}Bi_y)_{9.33}Ti_{18}O_{54}$: pre-reacted 10 h at 1200°C and sintered 20 min at 1320°C

y	y(anal.) (±0.007)	$f^{\#}$ (GHz)	*Permittivity*	τ_f (ppm/K)	$Q \times f$ (GHz)
0.100	0.088	4.335	83.0	20.2	7220
0.125	–	4.288	84.6	17.5	6690
0.150	–	4.162	89.8	17.1	6050
0.160	–	3.983	90.7	17.8	5470
0.170	0.141	4.090	90.8	16.9	5180
0.180	0.147	3.954	92.9	15.9	5010
0.190	0.161	3.978	92.9	15.4	4750
0.200	0.162	4.020	94.8	17.4	4390
0.225	–	3.929	94.6	24.2	3170
0.250	0.160	3.931	94.6	28.9	2800

. . .measurement frequency.

3.2. Bi incorporation in $Ba_{5.2}Nd_{8.53}Ti_{18}O_{54}$ ($x = 0.8$)

Microstructural investigations of the ceramics with nominal composition $Ba_{5.2}(Nd_{1-y}Bi_y)_{8.53}Ti_{18}O_{54}$ revealed the presence of a secondary phase which was identified as $Ba_6Ti_{17}O_{40}$ and/or $Ba_4Ti_3O_{30}$ (Fig. 5a and b). As with the Bi-substituted $Ba_4Nd_{9.33}Ti_{18}O_{54}$, [11] the concentration of the secondary phase increases initially with an increase in y. After exceeding $y = 0.15$ the concentration of the secondary phase increases significantly and, in addition, a Bi-rich phase appears, which is distributed at the grain boundaries (Fig. 5c).

The WDS analysis of the matrix grains in the $y \leq 0.15$ samples shows an increase in the concentration of bismuth up to $y = 0.14$ (Fig. 6). At this nominal composition $y_{anal.}$ temporarily stabilises at the value $y_{anal.} = 0.10$ (± 0.005). Any further increase in

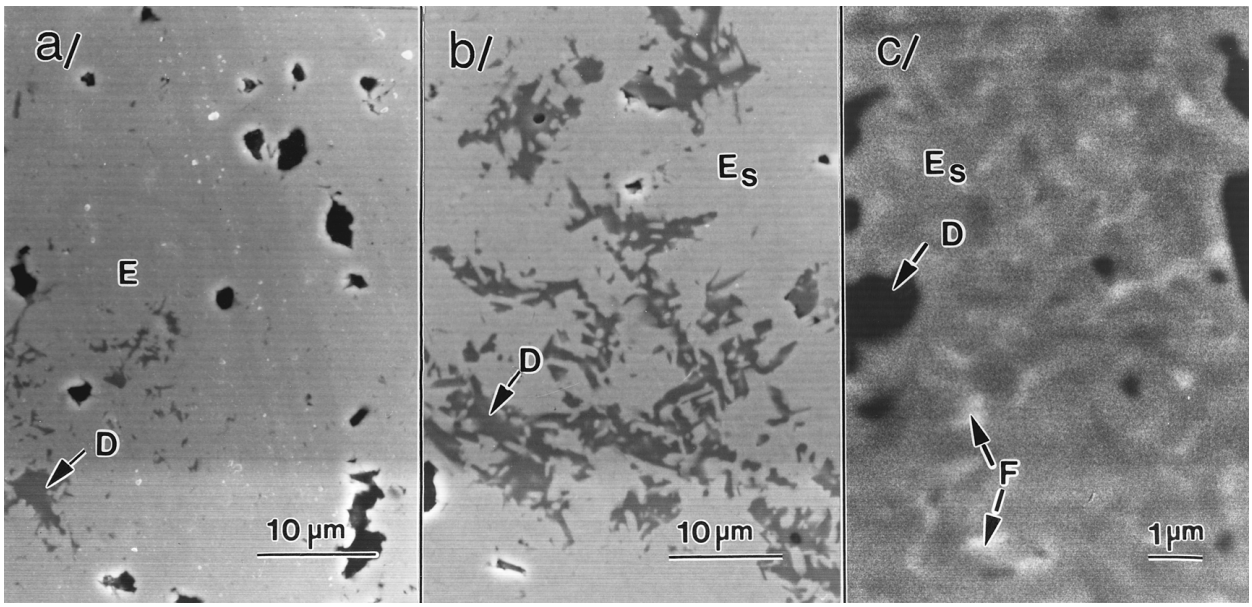

Figure 5 SEM micrographs of the polished surface of the ceramics with nominal composition $Ba_{5.2}(Nd_{1-y}Bi_y)_{8.53}Ti_{18}O_{54}$: pre-reacted 10 h at 1200°C and sintered 20 min at 1340°C – SEM images of $y = 0.10$ (a) and $y = 0.16$ (b) and back-scattered electron image of $y = 0.16$ (c)) (E. . .Bi-doped $Ba_{5.2}Nd_{8.53}Ti_{18}O_{54}$, E_s . . .saturated Bi-doped $Ba_{5.2}Nd_{8.53}Ti_{18}O_{54}$, D. . .Ba-polytitanate, F. . .Bi-rich phase).

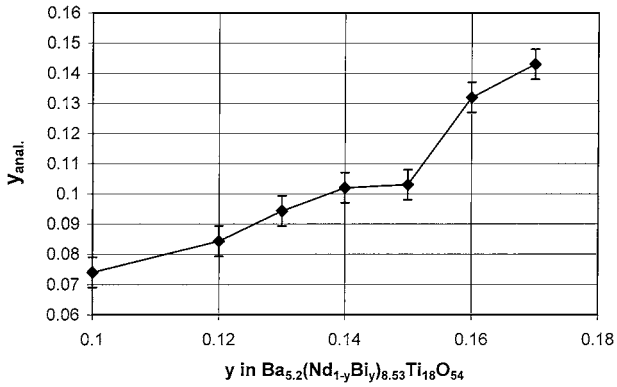

Figure 6 Analyzed (WDS) concentration of bismuth ($y_{anal.}$) in the grains of the matrix phase as a function of nominal bismuth concentration (y) in the $Ba_{5.2}(Nd_{1-y}Bi_y)_{8.53}Ti_{18}O_{54}$ ceramics: pre-reacted 10 h at 1200°C and sintered 20 min at 1340°C.

$y_{anal.}$ is believed to be a consequence of the presence of the grain boundary phase. Since the grains of the $Ba_{5.2}Nd_{8.53}Ti_{18}O_{54}$ ceramics are significantly smaller than the grains of the $Ba_4Nd_{9.33}Ti_{18}O_{54}$ (Fig. 7), accurate WDS microanalyses was possible only for the $y \leq 0.15$ samples. For $y > 0.15$ the Bi-rich grain-boundary phase interferes with the microanalyses of the matrix phase resulting in misleadingly high analytical concentrations of Bi. WDS analyses revealed no detectable changes in the composition of the matrix phase ($x_{anal.} = 0.82 \pm 0.05$).

The influence of the Bi substitution on the microwave dielectric properties is similar as to the case of $Ba_4Nd_{9.33}Ti_{18}O_{54}$ (Table II, Fig. 8). By increasing the concentration of bismuth the permittivity increases from 86.3 ($y = 0.1$) to 96.1 ($y = 0.16$) and remains approximately constant for $y > 0.16$ samples. The τ_f decreases from positive (10.3 ppm/K for $y = 0.1$) to negative values (−27 ppm/K for $y = 0.16$). After exceeding $y = 0.16$ the τ_f starts increasing with the increase in y.

TABLE II Compositional parameters and dielectric properties of the ceramics with nominal composition of $Ba_{5.2}(Nd_{1-y}Bi_y)_{8.53}Ti_{18}O_{54}$ pre-reacted 10 h at 1200°C and sintered 20 min at 1320°C

y	y(anal.) (±0.005)	$f^{\#}$ (GHz)	*Permittivity*	τ_f (ppm/K)	$Q \times f$ (GHz)
0.10	0.074	4.139	86.3	10.3	1260
0.12	0.084	4.097	87.2	−4.0	1010
0.13	0.094	4.060	90.6	−12.1	890
0.14	0.102	3.992	92.8	−13.2	780
0.15	0.103	4.008	93.8	−21.2	770
0.16	0.132	3.980	96.1	−27.0	700
0.17	0.143	3.982	95.8	−21.0	690

. . .measurement frequency.

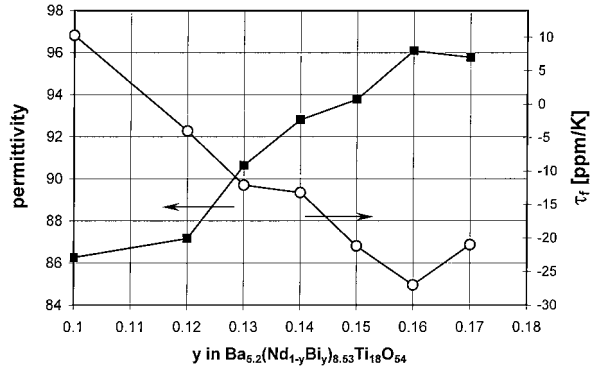

Figure 8 Permittivity and temperature coefficient of resonant frequency as a function of the of nominal bismuth concentration (y) in the $Ba_{5.2}(Nd_{1-y}Bi_y)_{8.53}Ti_{18}O_{54}$ ceramics pre-reacted 10 h at 1200°C and sintered 20 min at 1340°C.

Dielectric losses increase over the whole investigated range of y.

3.3. Bi incorporation in $Ba_{4.5}Gd_9Ti_{18}O_{54}$

The analyses of Bi-substituted $Ba_{4.5}Gd_9Ti_{18}O_{54}$ were made difficult due to the fact that during heat treatment the ceramics fail to densify and as a result maintain a

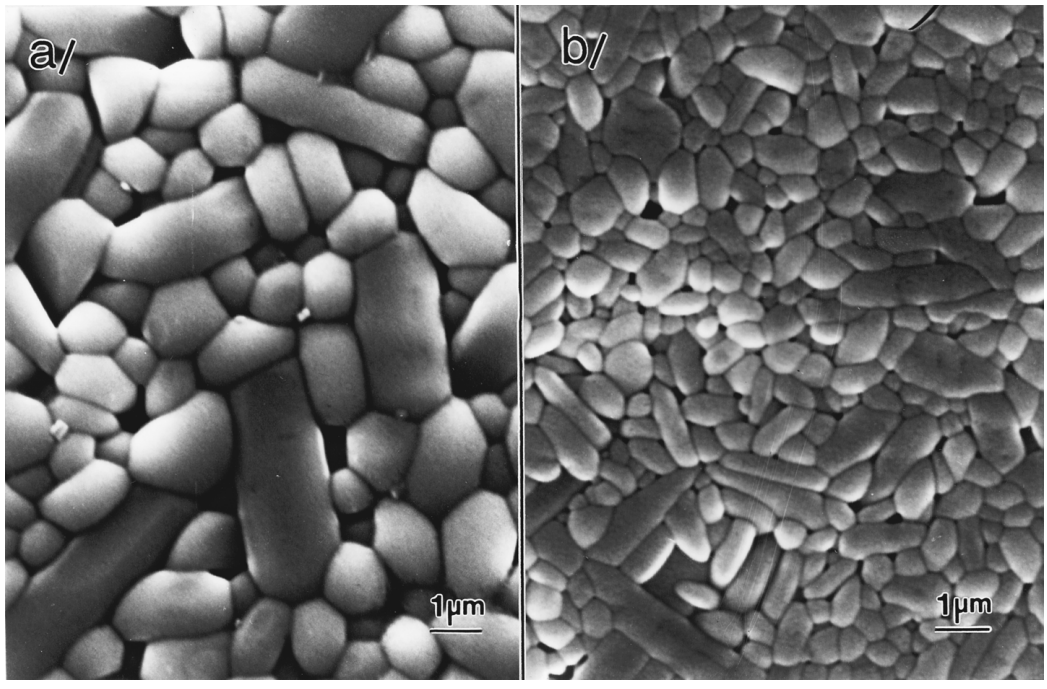

Figure 7 SEM images of thermally etched surface of $Ba_4Nd_{9.33}Ti_{18}O_{54}$ (a) and $Ba_{5.2}Nd_{8.53}Ti_{18}O_{54}$ (b) ceramics: sintered 20 h at 1400°C.

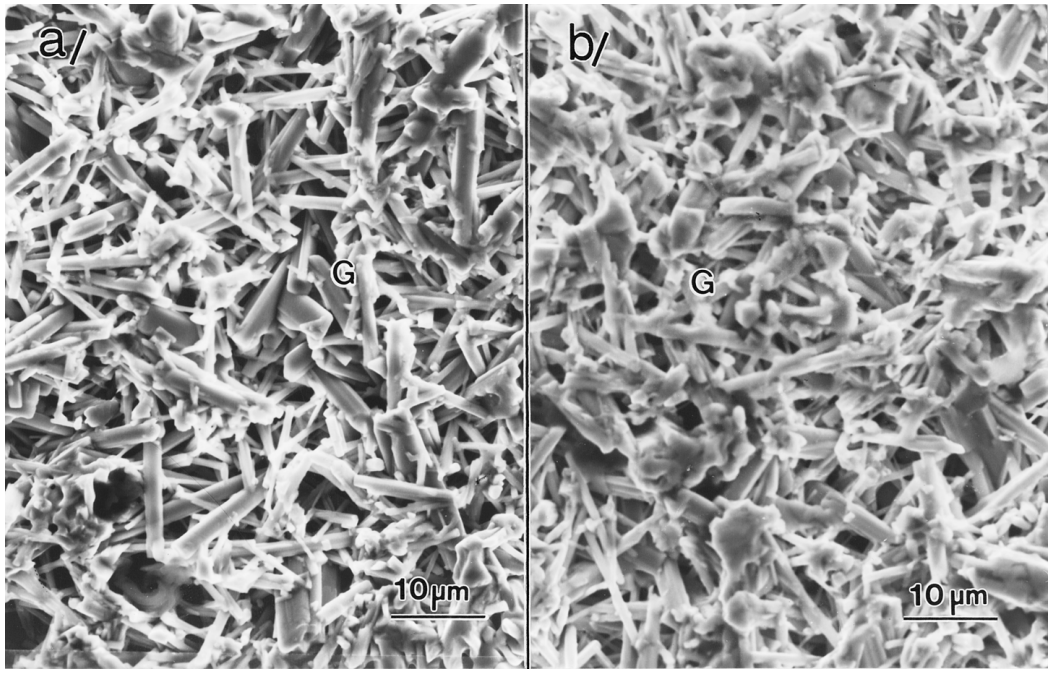

Figure 9 SEM images of the ceramics with nominal composition $Ba_{4.5}(Gd_{1-y}Bi_y)_9Ti_{18}O_{54}$: pre-reacted 10 h at 1150°C and sintered 20 min at 1340°C ($y = 0.03$ (a) and $y = 0.08$ (b)) (G. . .Bi-doped $Ba_{4.5}Gd_9Ti_{18}O_{54}$).

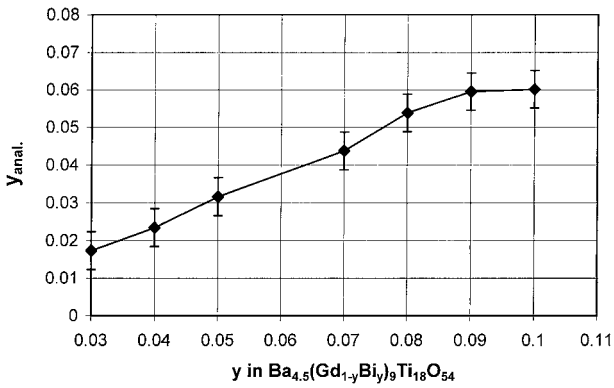

Figure 10 Analyzed (EDS) concentration of bismuth ($y_{anal.}$) in the grains of the matrix phase as a function of nominal bismuth concentration (y) in the $Ba_{4.5}(Gd_{1-y}Bi_y)_9Ti_{18}O_{54}$ ceramics: pre-reacted 10 h at 1150°C and sintered 20 min at 1340°C.

high degree of porosity. The same phenomenon was already observed by Wu *et al*. [13] in the (Ba, Sr) O-Sm_2O_3-TiO_2 system. It can be explained by the rapid growth rate of the highly anisometric crystallites. During their growth, they first come into contact and are then pushed away from one another. This result in an expansion of the ceramic sample and a decrease in the bulk density. The microstructure of the ceramic with the nominal composition $Ba_{4.5}(Gd_{1-y}Bi_y)_9Ti_{18}O_{54}$ and $y < 0.09$ appears as a conglomerate of homogeneously distributed needle-like crystallites (Fig. 9).

Because of the high degree of porosity, EDX rather than WDS analyses were performed. The analyzed concentration of bismuth in the grains of the matrix increases with y up to $y = 0.09$ where it reaches the value of $y_{anal.} = 0.06$ (± 0.005) (Fig. 10). Due to the high porosity no secondary phases can be seen in the microstructure, however, their presence cannot be excluded. A further increase in y does not influence the composition of the $Ba_{4.5}(Gd_{1-y}Bi_y)_9Ti_{18}O_{54}$-based phase but rather it induces the formation of dense areas in the matrix with a needle-like grain structure (Fig. 11a). EDX microanalyses performed on the dense areas revealed the presence of $Gd_2Ti_2O_7$ and a Ba-polytitanate phase (Fig. 11b), while the presence of the Bi-rich phase, which can be expected by analogy with the Nd-system, cannot be confirmed nor disproved. The influence of Bi incorporation in $Ba_{4.5}Gd_9Ti_{18}O_{54}$ on the dielectric properties was not analyzed because of the low density of the ceramic samples.

4. Discussion

Several common microstructural characteristics were revealed in the investigated systems. Firstly, in all the investigated systems a broad initial range of y exists where almost no changes in the microstructure can be observed. The only significant compositional variation is the continuous increase in the Bi concentration within the matrix grain, revealed by the microanalysis. Together with the studies performed on the $x = 1.5$ Nd analogue this fact demonstrates the correct explanation of the substitutional mechanisms for the investigated x- and R-range of $Ba_{6-x}R_{8+2x/3}Ti_{18}O_{54}$ solid solutions. The formation of the secondary phases within the initial y-range is a consequence of a loss of Bi during thermal treatment and can be avoided by the addition of a Bi excess to the nominal compositions. In the case of the Nd analogue, single-phase ceramics with the composition $Ba_{5.2}(Nd_{0.9}Bi_{0.1})_{8.53}Ti_{18}O_{54}$ and $Ba_4(Nd_{0.84}Bi_{0.16})_{89.33}Ti_{18}O_{54}$ were produced with 25% and 20% excess Bi_2O_3, respectively.

In the analyzed systems a critical y-value (y^{crit}) exists at which important changes in the microstructure and the dielectric properties occurred. Typically, at the y^{crit} the concentration of secondary phases significantly

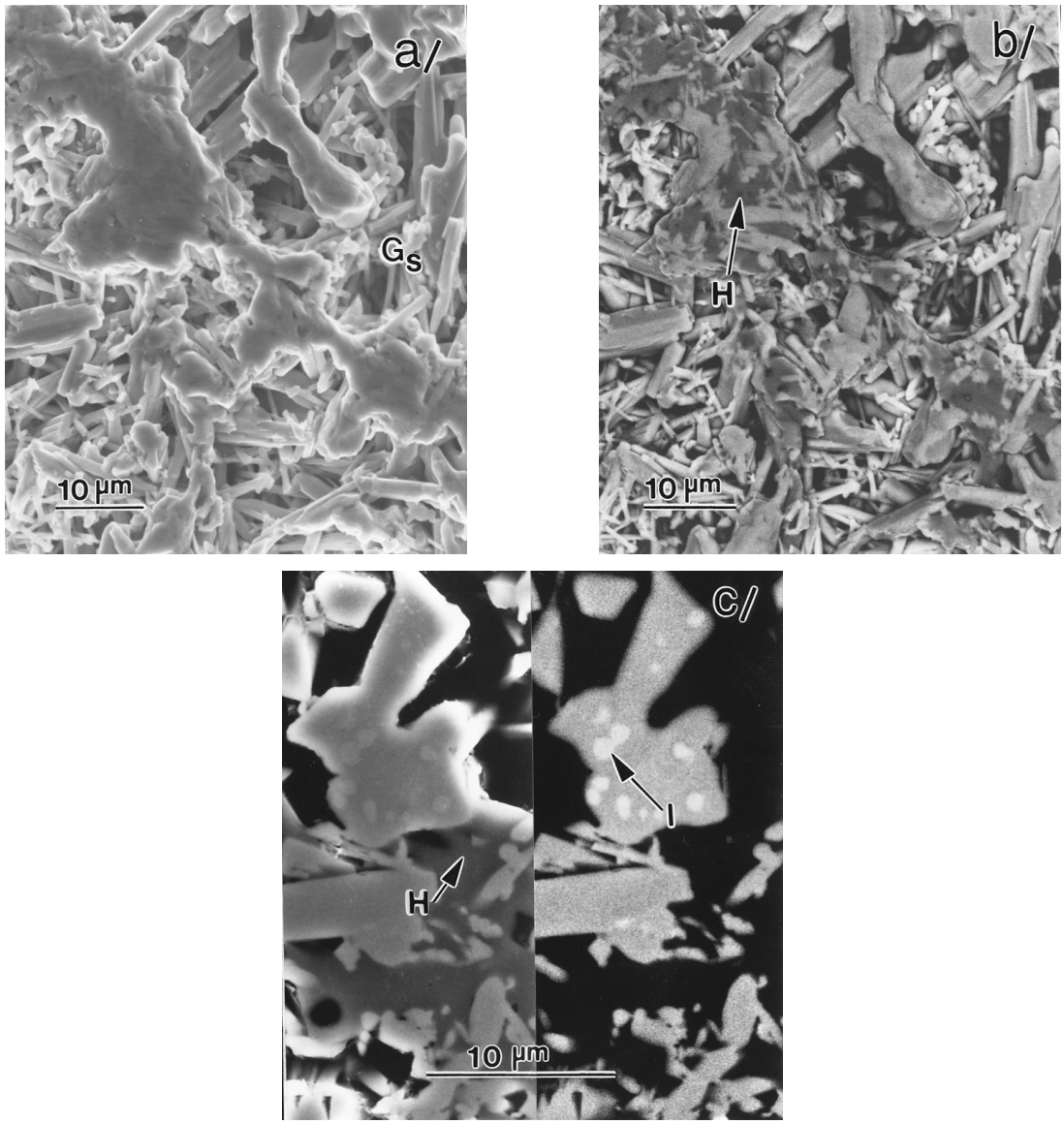

Figure 11 Micrographs of the polished surface of the ceramics with nominal composition $Ba_{4.5}(Gd_{1-y}Bi_y)_9Ti_{18}O_{54}$: pre-reacted 10 h at 1150°C and sintered 20 min at 1340°C – SEM images (a) of $y = 0.09$, and back-scattered image of $y = 0.09$ (b) and $y = 0.10$ (c – two different contrasts of the same area) (G_s . . . saturated Bi-doped $Ba_{4.5}Gd_9Ti_{18}O_{54}$, H. . .Ba- polytitanate, I. . . $Gd_2Ti_2O_7$).

increases and this is accompanied by the appearance of the Bi-rich phase at the grain boundaries. Dielectric properties also show abrupt changes at the same y^{crit}. Whereas for small values of y the permittivity shows a constant upward trend, it stops at y^{crit} and remains constant with any further increase in y. The temperature coefficient of the resonant frequency initially decreases but for the same y^{crit} the trend is altered. An important characteristic that coincides with the described phenomena relates to the composition of the matrix phase. Microanalyses clearly revealed that the concentration of Bi in the grains of the matrix increases only up to y^{crit}. A further increase in y does not influence the composition of the matrix, which shows that above y^{crit} the $Ba_{6-x}R_{8+2x/3}Ti_{18}O_{54}$ grains are already saturated with Bi. In fact, analyzed concentration of Bi in saturated $Ba_{6-x}R_{8+2x/3}Ti_{18}O_{54}$ grains represents a solid-solubility limit for Bi substitution of R in $Ba_{6-x}R_{8+2x/3}Ti_{18}O_{54}$ grains (y^{ss}). By exceeding the solid-solubility limit variations in the phase composition of the ceramics are induced which results in the abrupt changes in the dielectric properties.

The substitutional experiments proved that the solid-solubility limit of Bi in $Ba_{6-x}Nd_{8+2x/3}Ti_{18}O_{54}$ decreases with a decrease in x. As was shown by the EXAFS analyses, the substitution of Nd for Bi does not occur randomly over all the Nd-occupied sites but on one particular crystallographically-specific site only [12]. When all the Nd ions occupying this site are substituted a solid solubility limit appears and no further Bi substitution of Nd ions, remaining in the structure, is possible. Crystallographic analyses of $Ba_{6-x}R_{8+2x/3}Ti_{18}O_{54}$ structures showed that the Nd occupancy of this particular site in parent compositions decreases with the decrease in x, which explains the decrease in the y^{ss} occurring in the range from $x = 2.0$ to $x = 0.8$ of $Ba_{6-x}Nd_{8+2x/3}Ti_{18}O_{54}$. Compared to the $Ba_{6-x}Nd_{8+2x/3}Ti_{18}O_{54}$ system the Gd analogue exhibits a significantly lower y^{ss}. It is important to understand that $Ba_{4.5}Gd_9Ti_{18}O_{54}$ is the least stable representative in the family of $Ba_{6-x}R_{8+2x/3}Ti_{18}O_{54}$ compositions, [9] and as such, it is not able to accommodate higher concentrations of substituents.

TABLE III Compositional parameters and dielectric properties of Bi-saturated single-phase $Ba_{6-x}R_{8+2x/3}Ti_{18}O_{54}$ ceramics

					Undoped			Doped (compensated for Bi-loss)		
	x	x_{anal}	y^{crit}	y^{ss}.	*Permittivity*	τ_f (ppm/K)	$Q \times f$ (GHz)	*Permittivity*	τ_f (ppm/K)	$Q \times f$ (GHz)
$Ba_{6-x}Nd_{8+2x/3}Ti_{18}O_{54}$	2.0	1.9 (±0.05)	0.19	0.16 (±0.007)	84.0	56	10500	98.8	11.6	4800
	1.5*	1.5 (±0.03)	—	0.15 (±0.003)	86.2	81	7960	99	15	5500
	0.8	0.82 (±0.05)	0.15	0.10 (±0.005)	87.9	95	1890	93.8	11.1	1300
$Ba_{4.5}Gd_9Ti_{18}O_{54}$	1.5	1.5 (see lit. 9)	0.09	0.06 (±0.005)	76.1	−35	2050	—	—	—

* . . .from the lit. 11.

The dielectric properties as a function of Bi concentration were analysed and already discussed (Tables I and II and Figs 4 and 8). However, for an accurate comparison of the dielectric-property modification that can be achieved by the Bi incorporation in $Ba_{6-x}Nd_{8+2x/3}Ti_{18}O_{54}$, Bi-saturated single-phase ceramics were produced by using an excess of Bi_2O_3 to compensate for the loss of Bi. The permittivity of such samples was in all cases well above 90 (Table III) as a result of the high ionic polarizability of Bi. Interestingly, regardless of the τ_f of the parent compositions, all saturated samples exhibited a τ_f in the range of 11 to 15 ppm/K. For all investigated analogues the dielectric losses increased with increasing y, nevertheless, for high-x compositions the $Q \cdot f$-values remained at ∼5000 GHz, which is rather high for materials with a permittivity close to 100.

5. Conclusions

Substitutional experiments together with microstructural and dielectric property analyses showed that over the entire range of $Ba_{6-x}R_{8+2x/3}Ti_{18}O_{54}$ compositions bismuth ions incorporate into the crystal structure by substituting for rare-earth ions. The solid-solubility limit for this mechanism depends on the composition (x and R) of the $Ba_{6-x}R_{8+2x/3}Ti_{18}O_{54}$. The solid-solubility limit decreased with a decrease in the compositional parameter x in the $Ba_{6-x}Nd_{8+2x/3}Ti_{18}O_{54}$ system. It also decreased after the system was changed from the Nd to Gd analogue. When the solid-solubility limit was exceeded, abrupt changes in the microstructural and dielectric characteristics were induced. Typically, a significant amount of secondary phases was developed including a Bi-rich phase that concentrates at the grain boundaries. This was reflected in the dielectric properties. While up to the solid-solubility limit, permittivity increased and τ_f decreased: after exceeding the solid solubility limit the permittivity remained approximately constant and τ_f started to increase. Dielectric losses showed a continuous increase over the whole compositional range investigated.

References

1. R. G. MATVEEVA, M. B. VARFOLOMEEV and L. S. IL'YUHCHENKO, *Russ. J. Inorg. Chem.* **29** (1984) 17.
2. D. KOLAR, S. GABERSCEK, B. VOLAVSEK, H. S. PARKER and R. S. ROTH, *J. Solid State Chem.* **38** (1981) 158.
3. C. J. RAWN, D. P. BIRNIE, M. A. BRUCK, J. H. ENEMARK and R. S. ROTH, *J. Mater. Res.* **13** (1998) 187.
4. S. SKAPIN, D. KOLAR, D. SUVOROV and Z. SAMARDZIJA, *ibid.* **13** (1998) 1327.
5. M. B. VARFOLOMEEV, A. S. MIRONOV, V. S. KOSTOMAROV, L. A. GOLUBCHOVA and T. A. ZOLOTOVA, *Zh. Neorg. Khim.* **33** (1988) 1070 [*Translation Russ. J. Inorg. Chem.* **33** (1988) 607].
6. K. FUKUDA, R. KITOH and I. AWAI, *J. Mater. Res.* **10** (1995) 312.
7. H. OHSATO, T. OHHASHI, S. NISHIGAKI, T. OKUDA, K. SUMIA and S. SUZUKI, *Jpn. J. Appl. Phys.* **32** (1993) 4323.
8. T. NEGAS and P. K. DAVIES, *Ceram. Trans.* **53** (1995) 179.
9. M. VALANT, D. SUVOROV and D. KOLAR, *Jpn. J. Appl. Phys.* **35** (1996) 144.
10. D. SUVOROV, M. VALANT and D. KOLAR, *J. Mater. Sci.* **32** (1997) 6483.
11. M. VALANT, D. SUVOROV and D. KOLAR, *ibid.* **11** (1996) 928.
12. M. VALANT, I. ARČON, D. SUVOROV, A. KODRE, T. NEGAS and R. FRAHM, *ibid.* **12** (1997) 799.
13. J. M. WU, M. C. CHANG and P. C. YAO, *J. Amer. Ceram. Soc.* **73** (1990) 1599.

Received 19 April
and accepted 26 December 2000